



Risk estimation of soil slope stability problems

Guru Das¹ · Avijit Burman¹ · Abidhan Bardhan¹ · Sumit Kumar¹ · Shiva Shankar Choudhary¹ · Pijush Samui¹

Received: 25 October 2021 / Accepted: 12 January 2022 / Published online: 19 January 2022
© Saudi Society for Geosciences 2022

ABSTRACT

For successful design of any real-life engineering structures, it is important to quantify the risk of failure. Most of the geotechnical engineers find it suitable to define risk mathematically in terms of well-known metric called probability of failure. The inherent spatial variability of the soil strength parameters also makes the design of soil slopes suitable for stochastic interpretations. In the present study, probabilistic slope stability analysis has been performed for both, cohesive soil as well as cohesive frictional, i.e., $c - \phi$ soil. The estimation of the factor of safety of the soil slope has been carried out using ordinary method of slices. Probabilistic analysis has been carried out using the single random variable approach with the assumption that the cohesion and angle of internal friction of soils follow lognormal distribution. The variation in soil shear strength is taken into account with the help of statistical parameter known as coefficient of variation. The effect of the coefficient of variation, the spatial correlation length, and local averaging on the probability of failure and the factor of safety has been investigated. This phenomenon indicates a gradual variation of probability of failure with respect to the factor of safety at higher coefficient of variation values. The presented analyses can be used to determine the factor of safety of a soil slope for which the slope should be designed with a predefined probability of failure.

Keywords Slope Stability Analysis · Ordinary Method of Slices · Probabilistic Analysis · Spatial Correlation Length · Local Averaging · Coefficient of Variation · Probability of Failure

Introduction

Cautious investigations of the inherent stability of naturally occurring or man-made slopes are crucial to effective and successful engineering designs. The occurrences of slope

failures are numerous and different, in such a manner that an effort to model mathematically the mechanism of slope failures presents a challenging task for the engineers. What is observed, yet, is that numerous forms of instability initiate, or advance, by sliding along critical surfaces located inside the soil mass. Thus, it is evident that for many of the engineering uses (and also for a number of others), simple sliding soil mass models are sufficient. These slope stability analysis methods mainly comprise limit equilibrium method (LEM) (Bishop 1955; Fellenius 1936; Fredlund and Krahn, 1977; Janbu 1973; Morgenstern and Price 1965; Sarma 1973; Spencer 1967), strength reduction technique (SRT) based on finite element method (FEM) (Griffiths et al. 2009; Griffiths and Fenton 2000, 2004; Griffiths and Lane 1999; Griffiths and Yu 2015) and limit analysis method (Drucker and Prager 1952; Gao et al. 2014; Wai and Chen 1975; Wu 2015). Among them, the LEM has gained immense popularity all over the world because of its robustness and simplicity of concept.

LEM for stability analysis of soil slopes works on the principle of determination of an index, which divides the strength of soil in order to bring the soil slope on the verge

Responsible Editor: Zeynal Abiddin Erguler

✉ Pijush Samui
pijush@nitp.ac.in
Guru Das
gurud.pg19.ce@nitp.ac.in
Avijit Burman
avijit@nitp.ac.in
Abidhan Bardhan
abidhan@nitp.ac.in
Sumit Kumar
sumitk.phd19.ce@nitp.ac.in
Shiva Shankar Choudhary
shiva@nitp.ac.in

¹ Department of Civil Engineering, National Institute of Technology Patna, Patna, Bihar, India

of failure. This index is popularly known as factor of safety F_s . A state of limiting equilibrium in soil is achieved when the shear strength of the soil along the slip surface just equates to the disturbing forces trying to destabilize the slope. The LEM deals with principles of static equilibrium only. Most of the real-life slope stability problems are generally indeterminate in nature. LEM starts with an assumption of pre-fixed shape of the failure surface, i.e., circular, logarithmic spiral, parabolic, etc. LEM for the analysis of stability of soil slopes basically follows three approaches. One approach consists of satisfying the moment equilibrium only (Bishop 1955; Fellenius 1936), and another consists of satisfying the force equilibrium of individual slices and one more approach which satisfies both the overall moment equilibrium as well as force equilibrium (Morgenstern and Price 1965; Sarma 1973; Spencer 1967). A simple approach considering a general slip surface satisfying all the conditions of equilibrium was proposed by Sarma (1973). A generalized approach for stability analysis which conglomerates all the important aspects of earlier discussed methods was proposed by Fredlund and Krahn (1977). This method can be applied to slip surface of any geometry.

Identification of critical failure surface (CFS) and the determination of the associated minimum F_s of the slope is an integral part of any slope design based on LEM. A grid-based technique can be utilized in which F_s values are determined by using various positions of center of the slip circle with different radius values and finally choosing the circle with minimum F_s as the CFS. This method is limited to circular failure surfaces. For non-circular failure surfaces, various optimization methods were suggested which works toward finding a global minimum value of F_s . Baker and Garber (1978) suggested the use of variational formulations for optimization. Chen and Shao (1988), Nguyen (1985) adopted the simplex method for optimization as it is suitable for the case when gradient of global minimum is zero. Celestino and Duncan (1981) made use of alternating variable approach. These methods were based on the approach that global minimum will be found where the gradient of objective function is zero. Cheng (2003) suggested that global minimum can exist within another domain. With the increasing application of computers in engineering field, various heuristic optimization methods gained popularity. Kirkpatrick et al. (1983) suggested an optimization algorithm based on the heat treatment process termed as simulated annealing algorithm. Holand (1975) used the concept of genetic evolution of living beings and gave the genetic algorithm method. Further developments in the field of meta-heuristic optimization methods by Kennedy and Eberhart (1995) gave birth to particle swarm optimization (PSO) which is based on simulation involving simplified social models of flocking of birds in search of food source. Geem et al. (2001) and Lee and Geem (2005) used the musical method of search for a

perfect harmony state and developed a meta-heuristic algorithm known as simple harmony search method (SHM) for optimization. Cheng et al. (2007) improved the SHM method for application to complicated problems and developed the modified harmony search method. Dorigo (1992) used natural metaphors in solving optimization problems and is based on the optimization mechanism observed in Ants known as Ant-colony algorithm.

The traditional concept of F_s currently used by practicing geotechnical engineers is basically based on experience and has long been used in case of soil stability analysis. This F_s is applied to various problems of similar nature irrespective of the fact that every single one is different. It is basically a “one size fits all approach.” The deterministic approach of slope analysis does not take into account of the uncertainty of the input soil parameters which usually vary from one location to another. A better and more realistic approach would take into account the unpredictability of input parameters with respect to space. The unpredictability arises in the form of associated mathematical quantity termed as probability of failure (p_f) which is a measure of the uncertainties related to our inability to properly quantify the spatial variation of various soil properties and also various inaccuracies involved during estimation of these properties. Probability of failure (p_f) has become a very useful criterion for assessing the risk associated with an entity. The conflicting explanation of risk is a major cause of confusion and makes it difficult to quantify the acceptable risk. This acceptable risk means quantifying an acceptable p_f for slope analysis. Probabilistic slope stability analysis of soil mass has long attracted the attention of many scientists. A number of literary works are found which have contributed to this field’s further evolution. Matsuo and Kuroda (1974) concluded that soil properties can be treated as random variables. Whitman (1984) supported the need for estimation of risk in early stages of project. Phoon and Kulhawy (1999) utilized the statistical parameters to quantify geotechnical unpredictability. Griffiths and Fenton (2004) derived the relationship between p_f and F_s for undrained clay slope using the finite element method. Griffiths et al. (2009) determined the p_f in case of two-dimensional slopes and three-dimensional slope by making use of random finite element method. Griffiths and Yu (2015) observed a linear increment in undrained shear strength with increasing deepness. But most of the study was limited to classical techniques incorporating limit equilibrium approaches in it. The impact of variation basically of spatial nature, of soil properties was ignored, also ambiguity was found in the location of CFS along with ignorance of local averaging.

Machine learning is the new computer-based approach to analyze the stability of soil slopes as it utilizes the input data in order to predict the future trends. In this process, programmable algorithms are used to predict the

invisible patterns to make feasible decisions regarding design variables. A number of such algorithms such as SRLEM and BPNN have added to the realistic evaluation of soil slope stability problem. Chen et al. (2020) presented probabilistic evaluation of rock slope considering bi-planar sliding. BPNN is used to develop a surrogate model for factor of safety against bi-planar sliding. Zhang et al. (2021) presented the current geotechnical practices using deep learning algorithms. Extensive geotechnical applications of four major algorithms namely feedforward neural network (FNN), recurrent neural network (RNN), convolutional neural network (CNN), generative adversarial network (GAN) in the field of geotechnical engineering have been presented in recent literatures. Aladejare and Wang (2018) used Bayesian approach to indicate the correlation between c and ϕ and performed reliability-based slope stability analysis of rocks. Wang et al. (2020a, b) performed probabilistic slope stability analysis of Ashigong earth dam using a combination of MARS and GeoStudio software taking into account the uncertainty associated with soil parameters and water level fluctuation velocity. Wang et al. (2020a, b) performed stability analysis of Ashigong earth dam using XG-boost based reliability method and has been quite successful in predicting the failure probability. Further applications of machine learning algorithms in the field of slope stability analysis are highly warranted.

There have been numerous instances of catastrophes resulting from the failure of soil slopes. In most of the above cases, the design value of factor of safety was found to be greater than 1.5. One of the possible reasons could be the inability to take into account the uncertainty of input soil strength parameters. Modern mathematical tools of statistics and probability provide us with the arsenal to take into account the uncertainty of input variables. This study is a small initiative to use probabilistic tools to predict the failure probability and thus supplement the limit equilibrium method (LEM) based stability analysis of slopes. The procedure suggested in the paper can be utilized to improve and modify design codes for future slope stability analysis. In this study, the stability analysis of soil slope is carried out with special consideration toward the theoretical explanation of probabilistic approach of implementation procedure. This study aims at carrying out stability analysis of a cohesive soil slope and $c - \phi$ soil slope using classical techniques as well as using modern theories of statistics and probability. Single random variable approach is adopted in case of probabilistic analysis and the impact of using locally averaged soil properties on the is also studied. The p_f versus F_s curve attains linearity with negative slope as soon as ν approaches unity and greater than unity.

Methodology

Background

In this part, the theories, mathematical analysis and associated terminologies relevant to the study of probabilistic slope stability analysis are discussed. First of all, the classical approach for slope stability analysis of cohesive soil slope devised by Skempton (1948) based on the limit equilibrium approach is illustrated. Here, undrained cohesion has been treated as a random variable. After that a simple probabilistic analysis is performed using a single random variable perspective. The dependency of p_f with respect to coefficient of variation ν is also investigated in detail. The idea of local averaging is used to generate the random data. The effect of local averaging and spatial correlation length Θ on the desired output is also studied. In the next part, a $c - \phi$ soil slope is analyzed deterministically using the method of slices (Fellenius 1936). Further, probabilistic study of the $c - \phi$ slope is carried out and p_f has been determined for various cases such as keeping cohesion c constant while angle of internal friction ϕ has been treated as random variable and vice versa. The effect of ν on the p_f is also studied.

Random variable

In numerous analyses including components of arbitrariness, geotechnical engineers are regularly keen on some mathematical quantification related to the potential results instead of the actual results. So, to each entity in the sample space W a real number is allotted in a helpful manner in order to make estimate the probability of occurrence of the event under consideration. Mathematically, this approach deals with defining a real-valued function $Y : U \rightarrow R$ which, when certain parameters are satisfied, is called a random variable. These are of two types:

1. Discrete random variable: The random variable, which can take at most a fixed number of distinct values, is termed as discrete random variable.
2. Continuous random variable: A continuous random variable is the one which takes an endless number of conceivable outcomes. A continuous random variable is not characterized at particular values. Instead, it is specified over an interval of numerical values.

Choice of distributions

In geotechnical engineering, most of the time, situations arise in which it is necessary to deal with stationary random fields. Therefore, it is necessary to choose

a distribution that is truly sensible for the soil property which is going to be archetype. The Gaussian normal distribution, though a tremendously popular option, suffers from a huge disadvantage that its range varies from $-\infty$ to $+\infty$. For majority of soil parameters, for example, c or elastic modulus (E), negative values are unacceptable. So, for nonnegative soil properties, one such candidate is lognormal distribution which perfectly shows the distribution only on the positive side. In the upcoming sections, we are going to use lognormal as principal distribution for soil properties being used here.

Lognormal distribution

This distribution is termed as distribution of those properties in engineering which are strictly nonnegative specific to geotechnical engineering for example E , c , etc. Lognormal distribution is obtained from normal distribution by carrying out a nonlinear transformation. If H is a normally scattered random variable lying in the range $-\infty$ to $+\infty$, then $Y = \exp \{H\}$ will vary from $0 \leq y < \infty$. This implies that Y is lognormally distributed with mean μ and standard deviation σ . The probability density function of Y is given by

$$f(y) = \frac{1}{y\sigma_{\ln y}\sqrt{2\pi}} \exp \left\{ -\frac{1}{2} \left(\frac{\ln y - \mu_{\ln y}}{\sigma_{\ln y}} \right)^2 \right\} \text{ for } 0 < y < \infty \tag{1}$$

where $\mu_{\ln y}$ and $\sigma_{\ln y}^2$ are the mean and the variance of the normal distribution H , respectively. They are obtained as follows

$$\sigma_{\ln y}^2 = \ln \left(1 + \frac{\sigma_y^2}{\mu_y^2} \right) \tag{2}$$

$$\mu_{\ln y} = \ln(\mu_y) - \frac{1}{2}\sigma_{\ln y}^2 \tag{3}$$

Correlation function

The covariance function explains a little regarding the linear dependence between $Y(u')$ and $Y(u^*)$. A more feasible alternative to it will be correlation function. It is also positive definite in nature. It is given by

$$\rho(u', u^*) = \frac{C(u', u^*)}{\sigma_y(u')\sigma_y(u^*)} \tag{4}$$

where $\sigma_y(u')$ is the standard deviation of Y at the position u' . A numerical value of $\rho = \pm 1$ indicates perfect linear correlation either on positive or negative side.

Markov correlation function

It is the simplest function of all the functions applicable in geotechnical engineering. This function is formulated on the principle that the future is dependent on the present. Most of the existing body of work in engineering adopts this principle, Markov property is well applicable in today's era. The function is expressed in the form as defined below:

$$\rho(\tau) = \exp \left\{ -\frac{2\tau}{\theta} \right\} \tag{5}$$

The parameters τ and θ are the separation distance and correlation length, respectively. Correlation length is defined as the distance within which there exists a significant correlation between two points.

Variance function

Engineering properties generally consist of properties which are virtually local averages of some type. So, it is of significant interest for the engineers to study how the averages of random fields behave. A moving local average is expressed as

$$Y_U(u) = \frac{1}{U} \int_{u-\frac{U}{2}}^{u+\frac{U}{2}} Y(\eta) d\eta \tag{6}$$

where $Y_U(u)$ is the local average of $Y(u)$ over a window of width U centered at u . Local averaging generally influences the variances and the high-frequency components by reducing and damping out, respectively. But it preserves the mean of the random field. Now let us consider the variance part which is defined as

$$Var[Y_U(u)] = \sigma_Y^2 \gamma(U) \tag{7}$$

where $\gamma(U)$ is called the variance function, which tells how much variance is scaled down when $Y(u)$ is averaged over the length U . The variance function achieves a value of unity when the length U tends to 0. The variance function over an area $U_1 \times U_2$ in two dimensions is defined as

$$\gamma(U_1, U_2) = \frac{1}{U_1^2 U_2^2} \int_{-U_1}^{+U_1} \int_{-U_2}^{+U_2} (|U_1| - |\tau_1|)(|U_2| - |\tau_2|) \times \rho(\tau_1, \tau_2) d\tau_2 d\tau_1 \tag{8}$$

Considering quadrant symmetry, the above equation can be simplified as follows:

$$\gamma(U_1, U_2) = \frac{4}{U_1^2 U_2^2} \int_0^{U_1} \int_0^{U_2} (|U_1| - |\tau_1|)(|U_2| - |\tau_2|) \times \rho(\tau_1, \tau_2) d\tau_2 d\tau_1 \tag{9}$$

Now the two-dimensional variance function in terms of θ is given as

$$\gamma(U_1, U_2) = \frac{\theta_1^2 \theta_2^2}{4U_1^2 U_2^2} \left[\frac{2|U_1|}{\theta_1} + \exp \left\{ -\frac{2|U_1|}{\theta_1} \right\} - 1 \right] \times \left[\frac{2|U_2|}{\theta_2} + \exp \left\{ -\frac{2|U_2|}{\theta_2} \right\} - 1 \right] \tag{10}$$

where the symbols have their usual meanings. Eq. 10 can be evaluated using Gaussian quadrature.

Slope stability analysis

In this part, the determination of factor of safety F_s for undrained cohesive soil slope as well as for $c - \phi$ soil slope is discussed in brief. Stability analysis is carried out for both uniform soil as well as spatially varying soil. The expression of factor of safety for cohesive soil slope and for $c - \phi$ soil slope has been presented following moment equilibrium approach and the corresponding expressions have been depicted in the following text.

Evaluation of factor of safety (F_s):

Cohesive soil

The F_s is determined using the moment equilibrium approach. Let us consider a soil slope as shown in Fig. 1. For the slope shown in Fig. 1, F_s is determined using the moment equilibrium approach. The factor of safety of the cohesive soil slope is expressed as the ratio of resisting moment and the driving moment and is given by

$$F_s = \frac{c_u L_a R}{Wd} \tag{11}$$

where c_u = undrained cohesion L_a = Length of circular arc R = Radius of slip circle W = Weight of failure mass d = Lever Arm of the failure mass about center O of the slip circle.

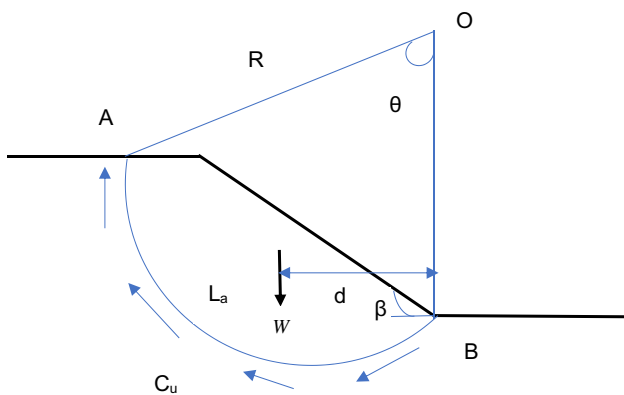


Fig. 1 Cohesive soil slope

Cohesive frictional ($c - \phi$) Soil

One of the earliest methods of analysis generally adopted for the evaluation of $c - \phi$ soil slope was ordinary method of slices. For the soil profiles where the effective ϕ is not found to be constant over the considered failure surface, the friction circle methodology cannot be used. The ordinary method of slices is the most appropriate one.

A cohesive frictional soil slope is as shown in Fig. 2. The expression of F_s for the slice under consideration is given by

$$F_s = \frac{cl + w \cos \alpha \tan \phi}{w \sin \alpha} \tag{12}$$

w = weight of slice, α is the angle made by the normal with the vertical.

Evaluation of probability of failure (p_f)

Cohesive Soil In this part, undrained cohesion c_u has been treated as random variable which leads to the following expression $c_u L_a R$ as random variable having lognormal distribution with statistical properties denoted by mean ($\mu_{c_u L_a R}$) and standard deviation ($\sigma_{c_u L_a R}$). The p_f value for the current case has been defined as the probability that the F_s value is less than 1. The p_f value is defined as

$$p_f = P[F_s < 1] = P \left[Z < \frac{\ln(Wd) - \mu_{\ln(c_u L_a R)}}{\sigma_{\ln(c_u L_a R)}} \right]. \tag{13}$$

The above expression denotes the expression for determination of p_f value in case of cohesive soil, where Z is the standard normal variate. This Z value is used to express a random variable with distribution given by $N(\mu, \sigma^2)$ to a standard form, i.e., having zero mean and unit variance using linear transformation.

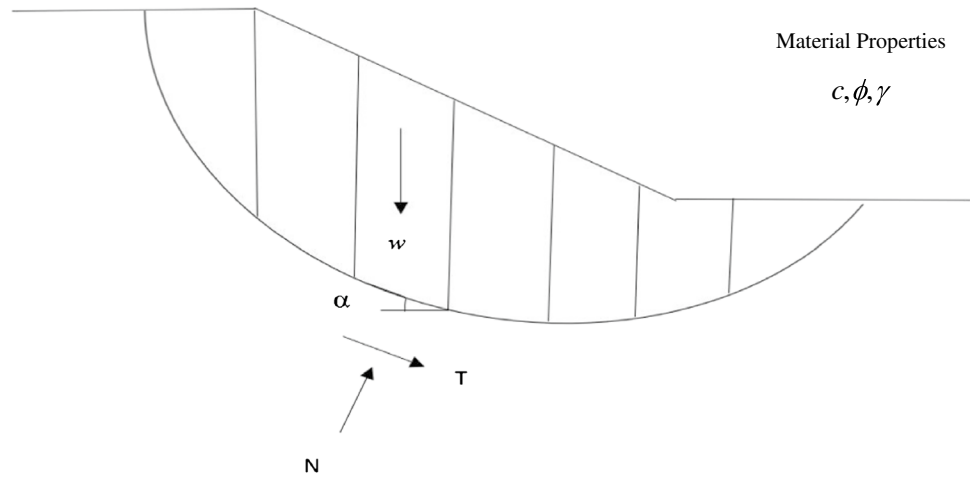
Cohesive Frictional ($c - \phi$) Soil In the present work, we are going to study how c and ϕ are going to affect the F_s if each of them is considered separately. First of all, we investigate the impact of cohesion upon associated F_s by keeping the ϕ value a constant and again the F_s is approximated using the following expression.

$$F_s = \frac{\sum cl}{\sum w \sin \alpha - \sum w \cos \alpha \tan \phi}. \tag{14}$$

Similarly, c to be constant, the expression for the F_s involved is given by

$$F_s = \frac{\sum w \cos \alpha \tan \phi}{\sum w \sin \alpha - \sum cl}. \tag{15}$$

Fig. 2 Cohesive frictional $c - \phi$ soil slope



Also, the F_s is determined considering both c and ϕ at a time using following expression and hence F_s is obtained.

$$F_s = \frac{F_R}{F_D} = \frac{\sum cl + \sum w \cos \alpha \tan \phi}{\sum w \sin \alpha} \tag{16}$$

where F_R and F_D represent the resisting/stabilizing and driving/destabilizing forces, respectively. Further, the value of p_f is determined considering c as the random variable for the first case, and then ϕ is treated as a random variable in the second case and further, both c and ϕ are treated as random variables and corresponding associated p_f is determined. The calculated p_f versus F_s graph is plotted for each case.

When only cohesion (c) is only considered as variable

In this case, the c is assigned lognormal distribution. Further, the p_f expression is derived as follows

$$p_f = P[F_s < 1] = P \left[Z < \frac{\ln(\sum w \sin \alpha - \sum w \cos \alpha \tan \phi) - \mu_{\ln(\sum cl)}}{\sigma_{\ln(\sum cl)}} \right] \tag{17}$$

Using Eq. 17, the p_f value is determined.

When only angle of internal friction (ϕ) is only considered as variable:

In this case, ϕ is assigned lognormal distribution. Further, the p_f expression is derived as follows

$$P[F_s < 1] = P \left[Z < \frac{\ln(\sum w \sin \alpha - \sum cl) - \mu_{\ln(\sum w \cos \alpha \tan \phi)}}{\sigma_{\ln(\sum w \cos \alpha \tan \phi)}} \right] \tag{18}$$

When both cohesion (c) and angle of internal friction (ϕ) are considered as variables:

Javankhoshdel and Bathurst (2016) gave analytical solution of p_f for cohesive soil by considering undrained strength S_u and unit weight γ as random variables. The analytical solution for $c - \phi$ soil assuming both cohesion c and angle of internal friction ϕ as lognormally distributed random variables doesn't seem to be mathematically feasible. When

logarithm is applied on the entire numerator term, i.e., ($F_R = \sum cl + \sum w \cos \alpha \tan \phi$) in Eq. 16, individual variation of c and ϕ cannot be considered. A logical and simple alternative would be to apply the variation on the entire F_R in Eq. 16 when the material parameters are assumed to vary lognormally. It should be kept in mind that the numerator term F_R actually represents the shear strength of the soil along the considered slip surface. Therefore, if the variation is applied on the entire numerator term F_R , it would include the effect of variation of the material parameters c and ϕ in a crude but simple manner. When Javankhoshdel and Bathurst (2016) carried out probabilistic slope stability analysis for a purely cohesive soil slope, the variation was applied on the undrained shear strength S_u which only depends on the cohesion c_u of the soil. When c and ϕ are both considered as lognormally distributed random variables, it seems logical to apply the variation on the shear strength along the slip surface. This simplification would allow us to obtain the design charts between F_s and p_f when the randomness of both c and ϕ is taken into consideration. Therefore, when both c and ϕ are assigned lognormal distribution, the expression of p_f expression becomes

$$\begin{aligned} P[F_s < 1] &= P \left[Z < \frac{\ln(\sum w \sin \alpha) - \mu_{\ln(\sum cl + \sum w \cos \alpha \tan \phi)}}{\sigma_{\ln(\sum cl + \sum w \cos \alpha \tan \phi)}} \right] \\ &= P \left[Z < \frac{\ln(\sum w \sin \alpha) - \mu_{\ln(F_R)}}{\sigma_{\ln(F_R)}} \right] \end{aligned} \tag{19}$$

Spatial variation of soil

The spatial variation of soil properties is taken into account using the concept of local averaging. Griffiths and Fenton (2004) advocated the use of local averaging subdivision method for developing random field involving single random

variable. The method can be useful in creating random distribution of any interested parameter (such as c and ϕ) over the domain of interest. Griffiths and Fenton (2004) have shown that the effect of local averaging on the lognormally distributed random variable can be mapped on a square element. Each element denotes a unique value of shear strength parameter (s). Now, the variance reduction factor for square element is determined by performing the numerical integration of variance reduction function. Now the expression of $\gamma(A)$ as a result of local averaging over an area element having area A is given by

$$\gamma(A) = \left(\frac{\sigma_{\ln(s)_a}}{\sigma_{\ln(s)}} \right)^2 \tag{20}$$

Therefore, the locally averaged value of the variable of interest, $\sigma_{\ln(s)_a}$ in this case can be obtained as

$$\sigma_{\ln(s)_a} = \sigma_{\ln(s)} \sqrt{\gamma(A)} \tag{21}$$

and assuming for two-dimensional isotropic case with equal θ in all directions, $\rho(\tau_1, \tau_2)$ is defined as

$$\rho(\tau_1, \tau_2) = \exp \left\{ -\frac{2}{\theta_{\ln(s)}} \sqrt{(\tau_1^2 + \tau_2^2)} \right\} \tag{22}$$

where τ_1 is the dissimilitude between the horizontal coordinates of two points τ_2 and is the disparity among the vertical coordinates of two points.

Considering a square-shaped element (refer to Fig. 3) having side length as a linear function of correlation length, let us denote a size parameter α such that area is depicted by $A = \alpha\theta_{\ln s} \times \alpha\theta_{\ln s}$. For square element, $\gamma(A)$ as per Vanmarcke (1983) is given by

$$\begin{aligned} \gamma(A) = & \frac{4}{(\alpha\theta_{\ln(s)})^4} \int_0^{\alpha\theta_{\ln(s)}} \int_0^{\alpha\theta_{\ln(s)}} (\alpha\theta_{\ln(s)} - x_1)(\alpha\theta_{\ln(s)} - x_2) \\ & \times \exp \left\{ -\frac{2}{\theta_{\ln(s)}} \sqrt{(x_1^2 + x_2^2)} \right\} dx_1 dx_2 \end{aligned} \tag{23}$$

where the symbols have their usual meanings. Using the above expression, we can determine values of variance reduction function for different values of size parameter and is shown in Fig. 4. Eq. 23 can be integrated numerically using Gaussian quadrature method as suggested by Griffiths and Fenton (2008). The variance reduction function $\gamma(A)$ can be calculated by discretizing the domain into square-shaped elements of size A . For, e.g., if the slope geometry is discretized as shown in Fig. 4, it can be seen that there are 20 square elements corresponding to the dimension H where H represents the height of slope which results in side of each square element being equal to $\frac{H}{20}$. While determining the variance reduction function for given size parameter α , we have considered square element with sides equal to $\alpha\theta_{\ln s}$ where $\theta_{\ln s}$ represents the spatial correlation length. Comparing these two parameters, the spatial correlation length is given by $\theta_{\ln s} = \frac{0.05H}{\alpha}$ and expressing in non-dimensional form, i.e., $\Theta = \frac{\theta_{\ln s}}{H} = \frac{\alpha}{0.05}$. Expressing spatial correlation length in dimensionless form adds to the simplicity of the problem and makes it possible to use the subsequent results to any size of the problem having same slope.

Using Eq. 23, the value of $\gamma(A)$ is obtained. From Eq. 20, it is now possible to determine the locally averaged value of standard deviation $\sigma_{\ln(s)_a}$. This value is placed in the respective expressions for probability of failure p_f . This results in different values of probability of failure. Spatial correlation length Θ is obtained by comparing the no. of elements and the dimensions of the soil slope. A plot of p_f against Θ for diverse values of v is obtained.

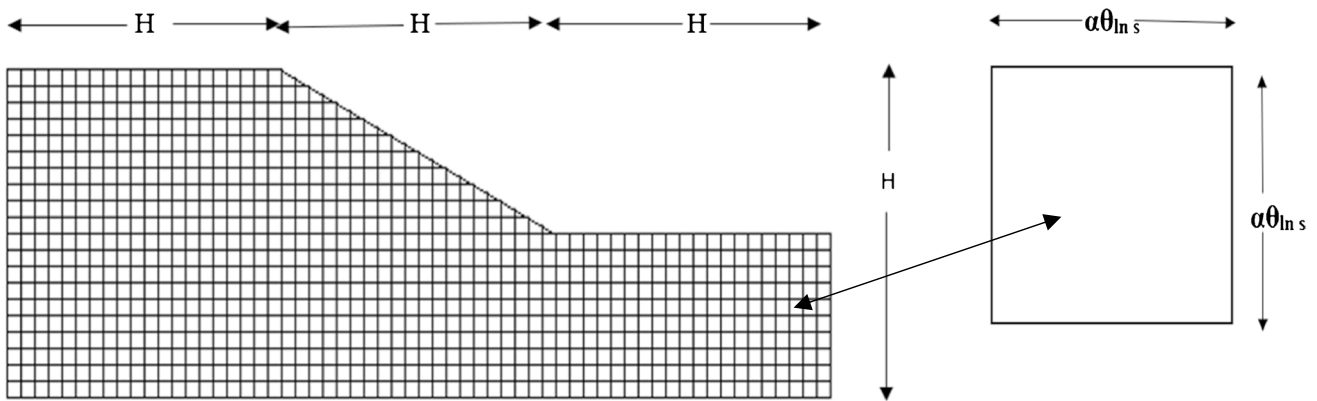
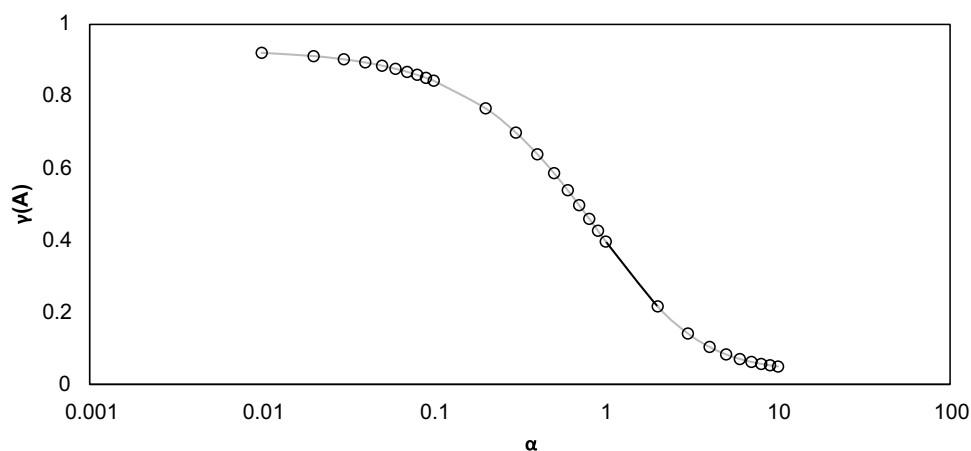


Fig. 3 Discretization of slope geometry into square-shaped elements of size A

Fig. 4 Variance reduction function as a function of size parameter



Results and discussion

This section consists of two parts. In the first part, single random variable approach is used which corresponds to spatial correlation length $\Theta = \infty$, i.e., uniform soil properties, while in the other part spatial variation of soil properties is considered through local averaging, i.e., smaller spatial correlation lengths Θ are considered. The variation of p_f with respect to F_s is studied for different values of coefficient of variation v . The variability of the material parameter throughout the soil domain is represented by considering various values of v . The obtained plots are useful to arrive at the design factor of safety F_s for any pre-fixed value of probability of failure (p_f) of the soil slope.

Variation of p_f vs. F_s for uniform Soil ($\Theta = \infty$)

Cohesive Soil

For an undrained cohesive soil slope, Griffiths and Fenton (2004) have shown that the factor of safety F_s against failure increases linearly with increase in the value of the undrained cohesion c_u . However, such deterministic estimation of F_s fails miserably to incorporate the effect of variability of c_u inside the slope. In case of soil domains where the properties show large variation, such incapability of considering the effect of variation of soil properties may lead to disastrous consequences. In such situations, it would be always desirable to take into consideration of the effect of soil variability in the slope analysis. In the present work, a cohesive soil slope of height $H = 5$ m, slope angle $\beta = 45^\circ$, saturated unit weight $\gamma_{sat} = 18.0$ kN/m³ (refer to Fig. 1) has been analyzed by considering undrained cohesion c_u to be lognormally distributed over the soil domain.

Fig. 5 shows the plot of probability of failure of p_f versus F_s for diverse values of coefficient of variation $v = v_{c_u}$ ranging between 0.0 and 8.0. Eq. 13 has been used to calculate p_f for different values of F_s obtained by considering resisting

moment $c_u L_a R$ as the mean input value. The p_f vs. F_s plots for v values are helpful in depicting the effect of variation of undrained cohesion c_u over the slope domain. The behavior observed at $v = 0.00$ is interesting as $\sigma_{\ln c_u L_a R} \rightarrow 0$ when $v \rightarrow 0$ which causes p_f to take only two extreme values either 0 or 1. Further, it is observed that with increasing F_s values after 1, the value of p_f increases as v increases. If a certain p_f is fixed as design requirement, the curves clearly depict that a higher F_s value must be achieved for a soil domain characterized by higher v signifying larger variation in its properties.

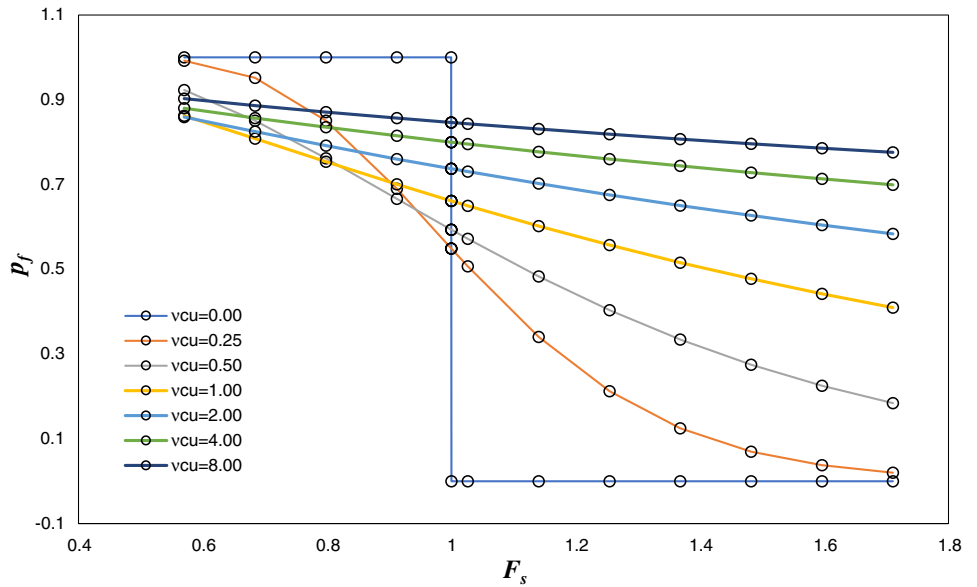
Cohesive–frictional ($c - \phi$) soil

Effect of variation of cohesion (c) Further, the study is carried forward by keeping ϕ constant and providing statistical properties to c using lognormal distribution specified mathematically by associated mean and standard deviation values. The value of ϕ is kept equal to 35° . F_s is determined by evaluating Eq. 14 and corresponding p_f is found out by making use of Eq. 17. The results shown in Fig. 6 is similar to earlier case with curves turning out to be steeper demonstrating how the variation of c influences the p_f versus F_s curves for $c - \phi$ soil slopes.

Effect of variation of angle of internal friction (ϕ)

The variation in ϕ has been introduced by means of an allotment of statistical properties to it assuming it as a random variable. The angle of internal friction ϕ is assumed to follow lognormal distribution characterized by the mean and standard deviation, while c is kept fixed at a value of 10 kN/m². The obtained results are shown in Fig. 7. In this case, F_s has been determined using Eq. 15 and the associated probability of failure p_f of the $c - \phi$ soil slope has been estimated by the use of Eq. 18. The curves depict how the variation of angle of internal friction ϕ affects the p_f values when the variation of soil properties has been simulated by using

Fig. 5 p_f vs F_s for undrained clay slope where c_u is a random variable



different $\nu = \nu_\phi$ values. Fig. 7 indicates that as ν increases, failure occurs at an inexorably more extensive range of F_s . This obtained result is further illustrated by the attainment of flat-shaped curves when ν increases gradually. For example, corresponding to ν value of 0.5, a F_s value of 1.3 yields a p_f value of 0.38. In other words, if the slope is designed for a p_f of 0.38, a minimum value of $F_s = 1.3$ is required.

Variability of both c and ϕ The variability of both c and ϕ is simulated by applying the variation on the shear strength F_R appearing in Eq. 16 as shown in Fig. 8. In this figure, the

symbol used to represent coefficient of variation of soil is $\nu_{c\phi} \approx \nu_{F_R}$. The factor of safety F_s of the slope is determined using Eq. 16 and corresponding p_f is evaluated from Eq. 19. If two previous cases are considered, where both c and ϕ were varied individually (refer to Figs. 6 and 7), it can be seen that the nature of variation of p_f vs. F_s follows similar trend. Although, the curves are comparatively less steep compared to the case when only c was treated as the random variable (refer to Fig. 6) as evident from the curves corresponding to coefficient of variation $\nu = 0.5$ in Figs. 6 and 8.

Fig. 6 p_f vs F_s in case of variation of cohesion c

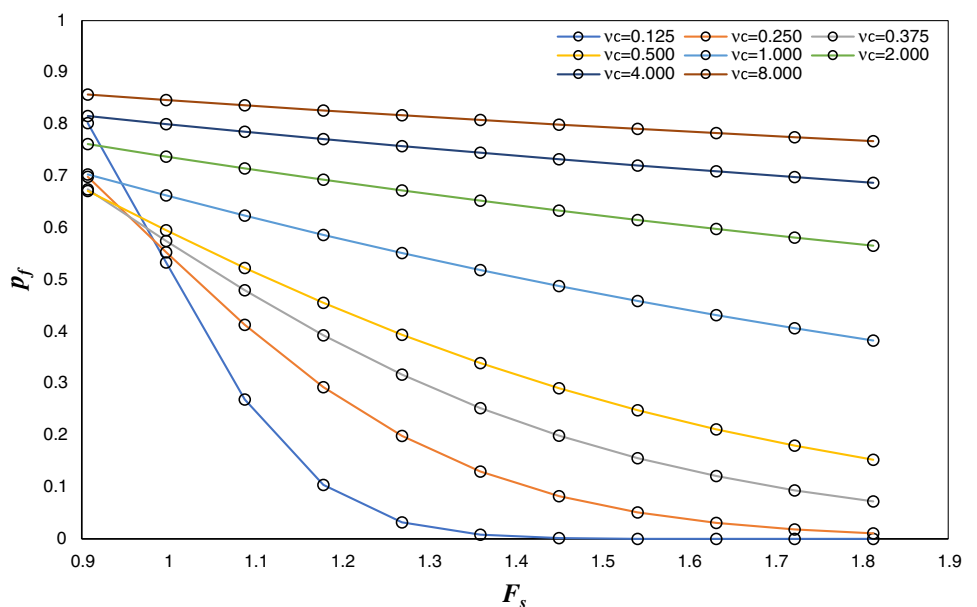
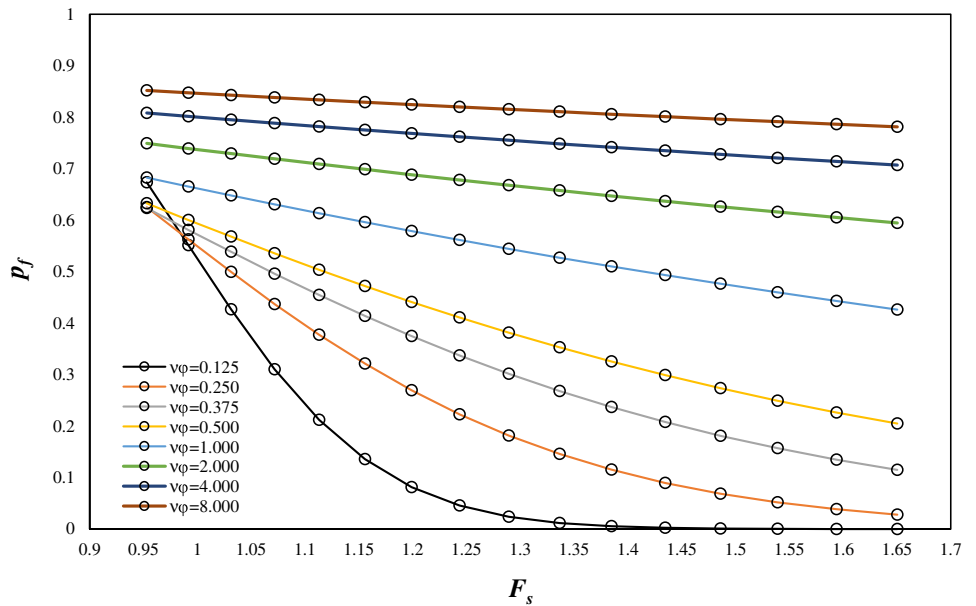


Fig. 7 p_f vs F_s in case of variation of friction angle ϕ



Spatially varying soil ($\Theta < \infty$)

Cohesive soil

In this section, the effect of correlation length on the probability of failure p_f of the soil slope is investigated for undrained cohesive soil slope characterized by material parameter c_u . However, in order to express the results in non-dimensional form, a modified correlation length $\Theta = \frac{\theta_{ln c}}{H}$ is defined. The advantage of non-dimensional form is that the results become independent of the units being used during calculation. The variation of p_f with Θ for different values of ν is shown in Fig. 9. The Θ is expressed in logarithmic form on abscissa and ordinate represents p_f . With reference to Fig. 9, the curve corresponding to $\nu = 0.42$ is almost a straight line, as not much

change is observed in the value of p_f with changing values of Θ . Apart from the straight line corresponding to $\nu = 0.42$, two types of curves are observed in Fig. 9, one is below the curve corresponding to $\nu = 0.42$ and the other above it. For the first set, that is below 0.42, positive slope of the curve is observed up to $\Theta > 1$. With an increase in the value of Θ , p_f value increases. On the other hand, the opposite nature is observed for the case when $\nu > 0.42$, i.e., negative slope is observed for most of curves. It is also evident that p_f value decreases with an increase in Θ . Similar behavior of curve is observed when the values of $\Theta > 1$ as the curves follow almost straight-line paths. The graph also depicts there is increase in p_f values with increase in ν for different Θ values.

The variation of p_f with F_s in case of using locally averaged statistics is illustrated in Fig. 10. This curve is plotted for constant

Fig. 8 p_f vs F_s in case of variation of both cohesion c and friction angle ϕ

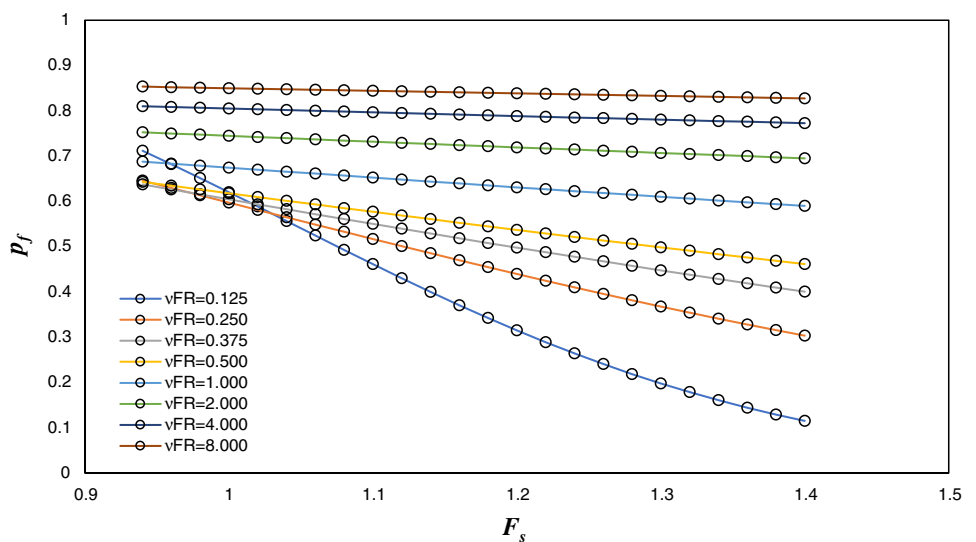
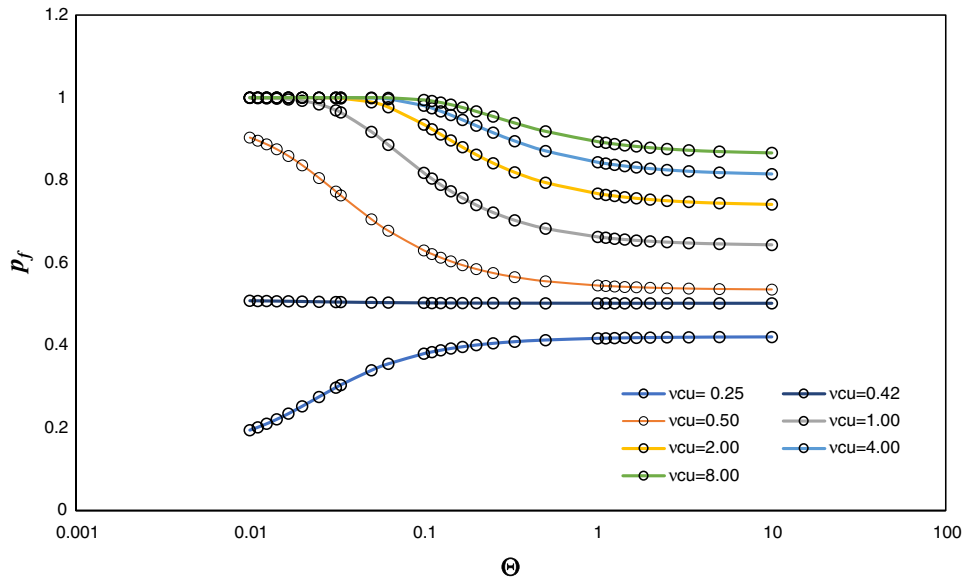


Fig. 9 p_f vs Θ for different values of ν in case of locally averaged statistics



value of $\nu = 0.50$ for different values of Θ ranging between 0 and ∞ . Most of the curves are similar except the one corresponding to $\Theta = 0$. In this case, i.e., for $\Theta = 0$, size parameter $\alpha \rightarrow \infty$, which results in $\gamma(A) \rightarrow 0$. In this case, $\sigma_{\ln(c_u L_u R_u)_A} \rightarrow 0$, which makes the value of Z either $-\infty$ or $+\infty$ and just provides scope for two values of p_f either 0 or 1. For other values of $\Theta > 0$, most of the curves are coinciding with each other and not much difference is observed, i.e., the curves corresponding to $\Theta = 10$ and that due to $\Theta = \infty$ are quite similar and almost no difference is observed in specific values.

Cohesive–frictional soil

Variation of c The effect of variation of Θ on the p_f is examined in the case of c assigned lognormal distribution having

a mean value of 7.5 kN/m^2 which corresponds to F_s value of 1.36. The value of ϕ is kept fixed at 35° . With an increase in Θ , the effect on p_f is not much pronounced due to the flattening of curves. As evident from the curves in Fig. 11, the p_f values increase with an increase in Θ .

The variation of p_f with F_s in case of using locally averaged statistics is illustrated in Fig. 12. This curve is plotted for constant value of $\nu = 0.50$ for different values of Θ ranging between 0 and ∞ . Most of the curves are similar except the one corresponding to $\Theta = 0$. In this case, i.e., for $\Theta = 0$, size parameter $\alpha \rightarrow \infty$, which results in $\gamma(A) \rightarrow 0$. In this case, $\sigma_{\ln(c_u L_u R_u)_A} \rightarrow 0$, which makes the value of Z either $-\infty$ or $+\infty$ and just provides scope for two values of p_f either 0

Fig. 10 p_f vs F_s for different values of Θ in case of local averaging

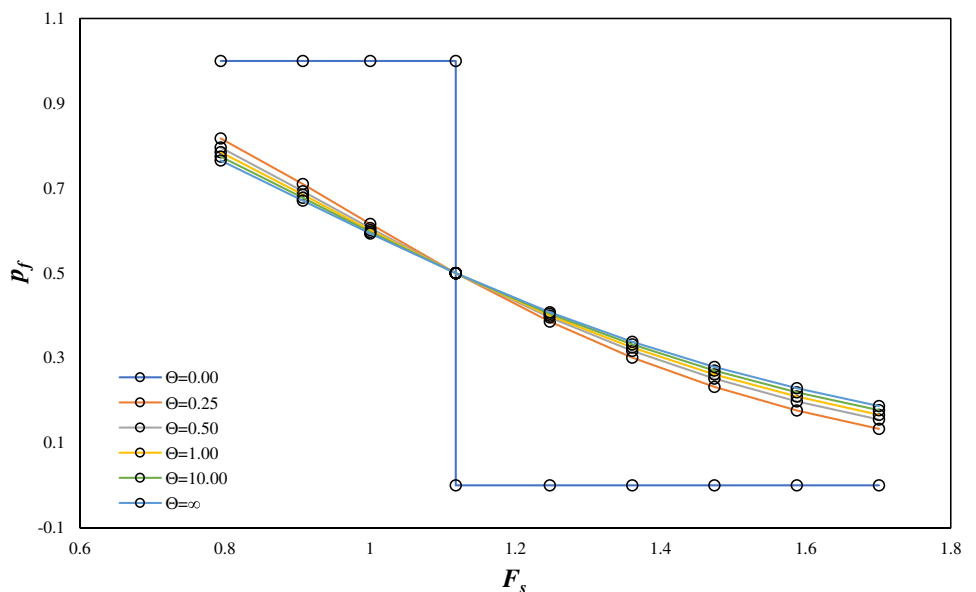
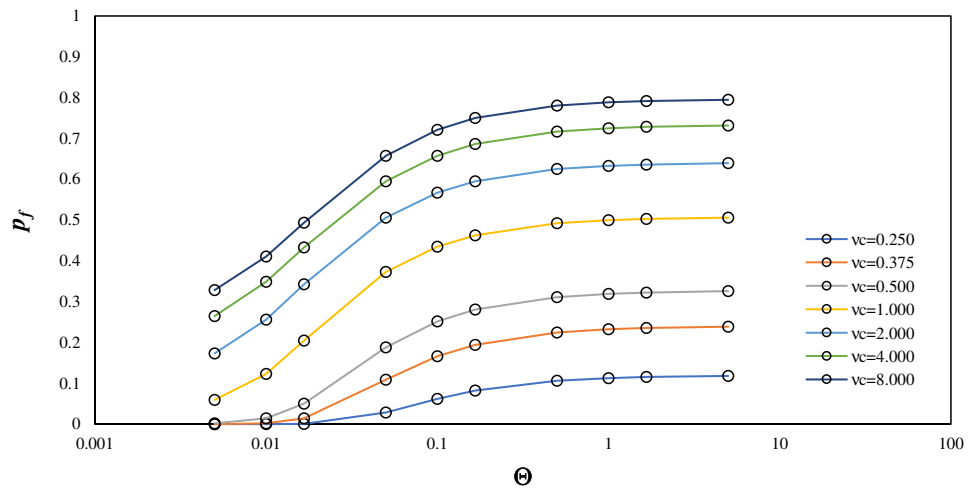


Fig. 11 p_f vs Θ considering local averaging



or 1. For nonzero values of spatial correlation length Θ , with increase in Θ the curves start to coincide with each other.

Variation of ϕ The effect of variation of Θ on the p_f is examined in the case of ϕ assigned lognormal distribution having a mean value of 34.9° which corresponds to F_s value of 1.13. The value of c is kept constant at 10 kN/m^2 . With an increase in Θ , the effect on p_f is not much pronounced due to the flattening of curves. As evident from the curves in Fig. 13, the p_f values increase with an increase in Θ .

The variation of p_f with F_s in case of using locally averaged statistics is illustrated in Fig. 14. This curve is plotted for constant value of $\nu = 0.50$ for different values of Θ ranging between 0 and ∞ . Most of the curves are similar except the one corresponding to $\Theta = 0$. In this case, i.e., for $\Theta = 0$, size parameter $\alpha \rightarrow \infty$, which results in $\gamma(A) \rightarrow 0$. In this case, $\sigma_{\ln(c_u L_\sigma R)_A} \rightarrow 0$, which makes the value of Z either $-\infty$

or $+\infty$ and just provides scope for two values of p_f either 0 or 1. For nonzero values of spatial correlation length Θ , with increase in Θ the curves start to coincide with each other.

Conclusions

Stability analysis of 1:1 cohesive soil slope and 2:1 $c - \phi$ soil slope is carried out using probabilistic approach. The LEM is used in both cases. Skempton (1948) approach has been followed for the case of cohesive soil while Fellenius (1936) approach has been followed in case of $c - \phi$ soil. The F_s was determined following the above-mentioned respective cases. Expressions for the p_f considering lognormal distribution of soil properties are also derived and p_f value in each case is obtained. A plot of p_f vs F_s is generated. Local averaging is performed over a square-shaped element and variance function is calculated using Markov correlation function for different values of scale of fluctuations/

Fig. 12 p_f vs F_s for different values of Θ in case of local averaging

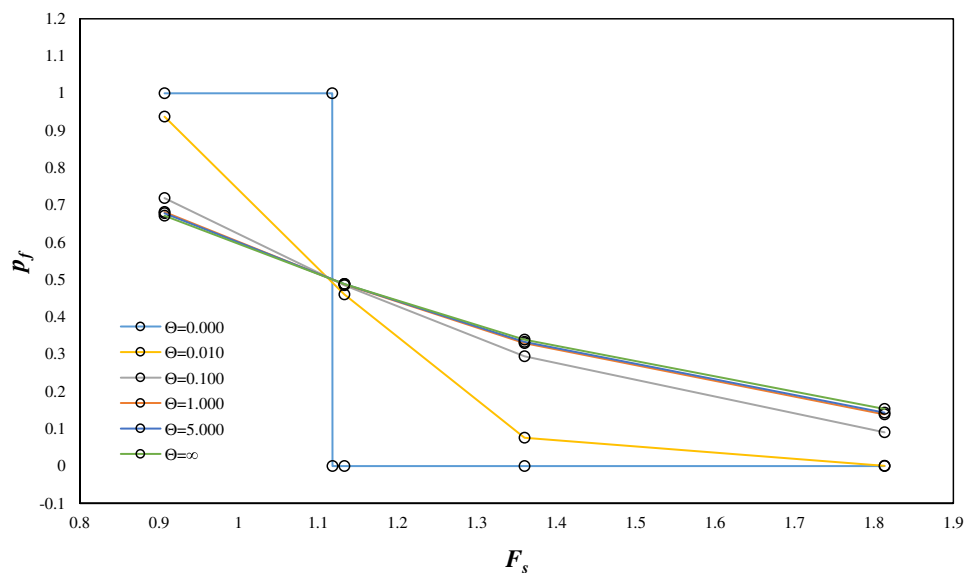
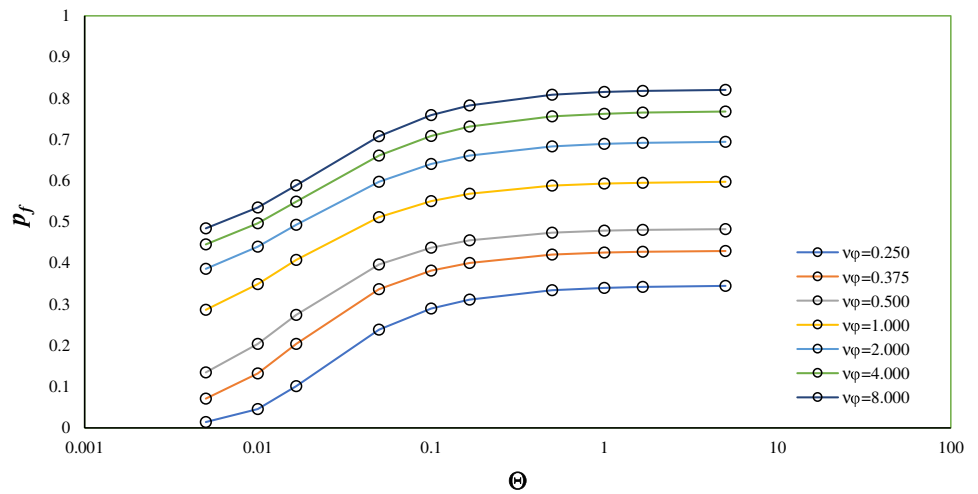


Fig. 13 p_f vs Θ considering local averaging



correlation length. Now the statistical soil parameters are modified after local averaging and using these modified values, p_f value is again calculated. A plot of p_f vs Θ and p_f vs F_s is generated. From these plots, following observations are made.

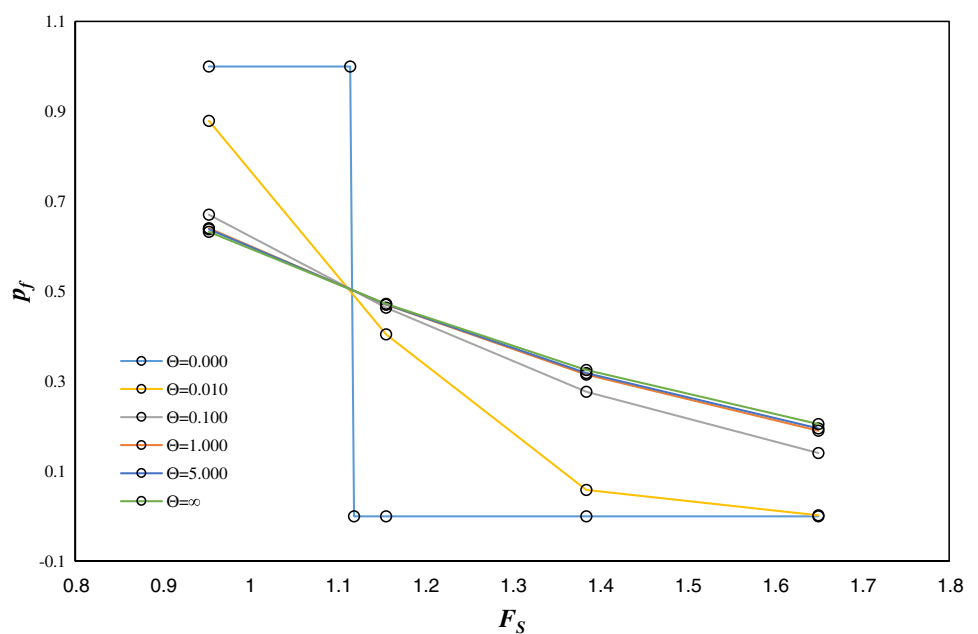
In case of earlier approaches, the idea of declaring a particular slope safe was limited to the attainment of a particular value of F_s preferably above 1.0, which is a quite ambiguous approach as we have seen that even if a higher magnitude of F_s is achieved, there is always an existence of finite magnitude of p_f . The variation of soil shear strength property is taken into cognizance by adopting the concept of ν which is helpful in depicting soil strength as lognormal distribution specified by associated parameters μ and σ .

It is observed that with an increment in the coefficient of variation ν , respective p_f increases for same value of F_s for

both cohesive and $c - \phi$ soil slopes. Similarly, for smaller p_f , F_s can be limited if value of ν is small, i.e., while designing for a given value of p_f , F_s should be provided as per the variation of soil properties governed by ν . The impact of Θ upon the p_f is discerned up to unit value of spatial correlation length after which their impact becomes negligible, i.e., not much change is observed in p_f with increasing correlation lengths. The study highlights the need for adopting a p_f based design approach of slopes. Such approach will drastically minimize the occurrences of frequent slope failures.

The limitations of the present study include a) the mathematical formulation for probabilistic analysis of soil slope has been able to well represent the separate effects of cohesion and friction, but the mathematical limitation to separate the cohesion and friction bound by logarithmic interpretation has hampered

Fig. 14 p_f vs F_s for different values of Θ in case of local averaging



the initiative. However, when the probabilistic analysis of $c - \phi$ soil has been carried out, the material parameters have been considered to be uncorrelated. There has been inherent inability to develop a relationship between cohesion and angle of internal friction so as to define a factor of safety in terms of single soil strength parameter which represents the effect of both cohesion and angle of internal friction. Nevertheless, the future scopes of this study may include a) in this study, ordinary method of slice has been used to estimate factor of safety of the slope. More rigorous slope stability analysis methods such as Bishop’s method, Janbu’s method, Morgenstern–Price method, may be used to estimate factor of safety of a slope and its subsequent probabilistic analysis; b) the effect of pore water pressure and earthquake loads can be incorporated and probabilistic study may be performed; c) a formulation may be suggested where the correlation between strength parameters (i.e., c and ϕ) are considered; d) the present study is based on the consideration of a specific geometric configuration of the slope. If the slope angle changes or provisions of berms are considered, the design charts will change. Therefore, it may be interesting to develop design charts involving probability of failure and the factor of safety of slope for another geometric configuration; and e) application of different machine learning algorithms such as artificial neural network (Asteris et al. 2021; Jalal et al. 2021; Kardani et al. 2021b; Onyelowe et al. 2021), adaptive neuro-fuzzy inference system (Jalal et al. 2021; Kaloop et al. 2021), gene-expression programming (Jalal et al. 2021) and extreme learning machine (Kardani et al. 2021a) can be used to perform reliability analyses of soil slopes considering uncertainties in soil characteristics.

APPENDIX

The probability of failure p_f against slope failure has been defined as the probability that the F_s value is less than 1. The derivation of the expression of p_f for different cases is shown below:

Cohesive Soil

For cohesive soil slope, the factor of safety F_s against failure is earlier mentioned in Eq. 11 and is given by

$$F_s = \frac{c_u L_a R}{Wd}. \tag{A1}$$

From Eq. A1, p_f is derived as follows:

$$p_f = P[F_s < 1] \\ = P\left[\frac{c_u L_a R}{Wd} < 1\right].$$

Taking logarithm on both sides, we get

$$= P[\ln(c_u L_a R) - \ln(Wd) < 0] \\ = P[\ln(c_u L_a R) < \ln(Wd)].$$

Subtracting $\mu_{\ln(c_u L_a R)}$ and dividing by $\sigma_{\ln(c_u L_a R)}$ on both sides, we get

$$= P\left[\frac{\ln(c_u L_a R) - \mu_{\ln(c_u L_a R)}}{\sigma_{\ln(c_u L_a R)}} < \frac{\ln(Wd) - \mu_{\ln(c_u L_a R)}}{\sigma_{\ln(c_u L_a R)}}\right] \\ = P\left[Z < \frac{\ln(Wd) - \mu_{\ln(c_u L_a R)}}{\sigma_{\ln(c_u L_a R)}}\right]. \tag{A2}$$

Cohesive Frictional Soil

In case of cohesive frictional, i.e., $c - \phi$ soil, different cases are considered in which soil properties such as cohesion and angle of internal friction are treated as lognormally distributed random variables. The respective expressions for factor of safety F_s against failure and the associated probability of failure are as described below.

For cohesion

In this case, the cohesion parameter is assigned lognormal distribution. The factor of safety F_s against failure is earlier mentioned in Eq. 14 and is given by

$$F_s = \frac{\sum cl}{\sum w \sin \alpha - \sum w \cos \alpha \tan \phi}. \tag{A3}$$

Further, the probability of failure p_f expression from A3 is derived as follows

$$p_f = P[F_s < 1] \\ = P\left[\frac{\sum cl}{\sum w \sin \alpha - \sum w \cos \alpha \tan \phi} < 1\right] \\ = P[\ln(\sum cl) - \ln(\sum w \sin \alpha - \sum w \cos \alpha \tan \phi) < 0] \\ = P[\ln(\sum cl) < \ln(\sum w \sin \alpha - \sum w \cos \alpha \tan \phi)].$$

Subtracting $\mu_{\ln(\sum cl)}$ and dividing by $\sigma_{\ln(\sum cl)}$, we get

$$= P\left[\frac{\ln(\sum cl) - \mu_{\ln(\sum cl)}}{\sigma_{\ln(\sum cl)}} < \frac{\ln(\sum w \sin \alpha - \sum w \cos \alpha \tan \phi) - \mu_{\ln(\sum cl)}}{\sigma_{\ln(\sum cl)}}\right] \\ = P\left[Z < \frac{\ln(\sum w \sin \alpha - \sum w \cos \alpha \tan \phi) - \mu_{\ln(\sum cl)}}{\sigma_{\ln(\sum cl)}}\right]. \tag{A4}$$

For angle of internal friction

In this case, the angle of internal friction is assigned lognormal distribution. The factor of safety F_s against failure is earlier mentioned in Eq. 15 and is given by

$$F_s = \frac{\sum w \cos \alpha \tan \phi}{\sum w \sin \alpha - \sum cl} \tag{A5}$$

Further, the probability of failure p_f expression from A5 is derived as follows

$$\begin{aligned} p_f &= P[F_s < 1] \\ &= P\left[\frac{\sum w \cos \alpha \tan \phi}{\sum w \sin \alpha - \sum cl} < 1\right] \\ &= P\left[\ln\left(\sum w \cos \alpha \tan \phi\right) - \ln\left(\sum w \sin \alpha - \sum cl\right) < 0\right] \\ &= P\left[\ln\left(\sum w \cos \alpha \tan \phi\right) < \ln\left(\sum w \sin \alpha - \sum cl\right)\right]. \end{aligned}$$

Subtracting $\mu_{\ln(\sum w \cos \alpha \tan \phi)}$ and dividing by $\sigma_{\ln(\sum w \cos \alpha \tan \phi)}$, we get

$$\begin{aligned} &= P\left[\frac{\ln(\sum w \cos \alpha \tan \phi) - \mu_{\ln(\sum w \cos \alpha \tan \phi)}}{\sigma_{\ln(\sum w \cos \alpha \tan \phi)}} < \frac{\ln(\sum w \sin \alpha - \sum cl) - \mu_{\ln(\sum w \cos \alpha \tan \phi)}}{\sigma_{\ln(\sum w \cos \alpha \tan \phi)}}\right] \\ &= P\left[Z < \frac{\ln(\sum w \sin \alpha - \sum cl) - \mu_{\ln(\sum w \cos \alpha \tan \phi)}}{\sigma_{\ln(\sum w \cos \alpha \tan \phi)}}\right]. \end{aligned} \tag{A6}$$

For both cohesion and angle of internal friction

In this case, both cohesion and angle of internal friction are assigned lognormal distribution. The factor of safety F_s against failure p_f is earlier mentioned in Eq. 16 and is given by

$$F_s = \frac{\sum cl + \sum w \cos \alpha \tan \phi}{\sum w \sin \alpha} \tag{A7}$$

Further, the probability of failure p_f expression from A7 is derived as follows

$$\begin{aligned} p_f &= P[F_s < 1] \\ &= P\left[\frac{\sum cl + \sum w \cos \alpha \tan \phi}{\sum w \sin \alpha} < 1\right] \\ &= P\left[\ln\left(\sum cl + \sum w \cos \alpha \tan \phi\right) - \ln\left(\sum w \sin \alpha\right) < 0\right] \\ &= P\left[\ln\left(\sum cl + \sum w \cos \alpha \tan \phi\right) < \ln\left(\sum w \sin \alpha\right)\right]. \end{aligned}$$

Subtracting $\mu_{\ln(\sum cl + \sum w \cos \alpha \tan \phi)}$ and dividing by $\sigma_{\ln(\sum cl + \sum w \cos \alpha \tan \phi)}$, we get

$$\begin{aligned} &= P\left[\frac{\ln(\sum cl + \sum w \cos \alpha \tan \phi) - \mu_{\ln(\sum cl + \sum w \cos \alpha \tan \phi)}}{\sigma_{\ln(\sum cl + \sum w \cos \alpha \tan \phi)}} < \frac{\ln(\sum w \sin \alpha) - \mu_{\ln(\sum cl + \sum w \cos \alpha \tan \phi)}}{\sigma_{\ln(\sum cl + \sum w \cos \alpha \tan \phi)}}\right] \\ &= P\left[Z < \frac{\ln(\sum w \sin \alpha) - \mu_{\ln(\sum cl + \sum w \cos \alpha \tan \phi)}}{\sigma_{\ln(\sum cl + \sum w \cos \alpha \tan \phi)}}\right] = P\left[Z < \frac{\ln(\sum w \sin \alpha) - \mu_{\ln(F_R)}}{\sigma_{\ln(F_R)}}\right]. \end{aligned} \tag{A8}$$

Declarations

Conflict of interest The authors declare that there is no conflict of interest.

REFERENCES

Aladejare AE, Wang Y (2018) Influence of rock property correlation on reliability analysis of rock slope stability: from property characterization to reliability analysis. *Geosci Front* 9(6):1639–1648

Asteris PG, Mamou A, Hajihassani M, Hasanipanah M, Koopialipour M, Le T-T, Kardani N, Armaghani DJ (2021) Soft computing based closed form equations correlating L and N-type Schmidt hammer rebound numbers of rocks. *Transp Geotech* 100588

Baker R, Garber M (1978) Theoretical analysis of the stability of slopes. *Geotechnique* 28(4):395–411

Bishop AW (1955) The use of the slip circle in the stability analysis of slopes. *Geotechnique* 5(1):7–17

Celestino TB, Duncan JM (1981) Simplified search for non-circular slip surface. *Proceedings, 10th International Conference on Soil Mechanics and Foundation Engineering, International Society for Soil Mechanics and Foundation Engineering, Stockholm, AA Balkema, Rotterdam, Holland* 3, 391–394

Chen L, Zhang W, Gao X, Wang L, Li Z, Böhlke T, Perego U (2020) Design charts for reliability assessment of rock bedding slopes stability against bi-planar sliding: SRLEM and BPNN approaches. *Georisk: Assessment and Management of Risk for Engineered Systems and Geohazards*, 1–16

Chen Z-Y, Shao C-M (1988) Evaluation of minimum factor of safety in slope stability analysis. *Can Geotech J* 25(4):735–748

Cheng YM (2003) Location of critical failure surface and some further studies on slope stability analysis. *Comput Geotech* 30(3):255–267

Cheng YM, Li L, Chi SC (2007) Performance studies on six heuristic global optimization methods in the location of critical slip surface. *Comput Geotech* 34(6):462–484

Dorigo M (1992) Optimization, learning and natural algorithms. Ph. D. Thesis, Politecnico Di Milano.

Drucker DC, Prager W (1952) Soil mechanics and plastic analysis or limit design. *Q Appl Mathe* 10(2):157–165

Fellenius W (1936) Calculation of stability of earth dam. *Transactions. 2nd Congress Large Dams, Washington, DC, 1936*, 4, 445–462

Fenton GA, Griffiths DV (2008) Risk assessment in geotechnical engineering (Vol. 461). John Wiley & Sons. New York

Fredlund DG, Krahn J (1977) Comparison of slope stability methods of analysis. *Can Geotech J* 14(3):429–439

Gao Y, Zhu D, Zhang F, Lei GH, Qin H (2014) Stability analysis of three-dimensional slopes under water drawdown conditions. *Can Geotech J* 51(11):1355–1364

- Geem ZW, Kim JH, Loganathan GV (2001) A new heuristic optimization algorithm: harmony search. *Simulation* 76(2):60–68
- Griffiths DV, Fenton GA (2000) Influence of soil strength spatial variability on the stability of an undrained clay slope by finite elements. In *Slope stability 2000* (pp. 184–193)
- Griffiths DV, Fenton GA (2004) Probabilistic slope stability analysis by finite elements. *J Geotech Geoenviron Eng* 130(5):507–518
- Griffiths DV, Huang J, Fenton GA (2009) On the reliability of earth slopes in three dimensions. *Proc R Soc A: Mathe Phys Eng Sci* 465(2110):3145–3164
- Griffiths DV, Lane PA (1999) Slope stability analysis by finite elements. *Geotechnique* 49(3):387–403
- Griffiths DV, Yu X (2015) Another look at the stability of slopes with linearly increasing undrained strength. *Géotechnique* 65(10):824–830
- Holand JH (1975) *Adaptation in Natural and Artificial Systems* 1975. University of Michigan Press, Ann Arbor, Mich
- Jalal FE, Xu Y, Iqbal M, Javed MF, Jamhiri B (2021) Predictive modeling of swell-strength of expansive soils using artificial intelligence approaches: ANN, ANFIS and GEP. *J Environ Manag* 289:112420
- Janbu N (1973) Slope stability computations—Embankment—Dam Engineering, Casagrande Volume. John Wiley and Sons, New York, pp 47–86
- Javankhoshdel S, Bathurst RJ (2016) Influence of cross correlation between soil parameters on probability of failure of simple cohesive and $c-\phi$ slopes. *Can Geotech J* 53(5):839–853
- Kalooop MR, Bardhan A, Kardani N, Samui P, Hu JW, Ramzy A (2021) Novel application of adaptive swarm intelligence techniques coupled with adaptive network-based fuzzy inference system in predicting photovoltaic power. *Renew Sustain Energy Rev* 148:111315
- Kardani N, Bardhan A, Roy B, Samui P, Nazem M, Armaghani DJ, Zhou A (2021) A novel improved Harris Hawks optimization algorithm coupled with ELM for predicting permeability of tight carbonates. *Eng Comput* 1–24
- Kardani N, Zhou A, Shen S-L, Nazem M (2021) Estimating unconfined compressive strength of unsaturated cemented soils using alternative evolutionary approaches. *Transp Geotech* 29:100591
- Kennedy J, Eberhart R (1995) Particle swarm optimization. In *Proceedings of ICNN'95-international conference on neural networks* (Vol. 4, pp. 1942–1948). IEEE
- Kirkpatrick S, Gelatt CD, Vecchi MP (1983) Optimization by simulated annealing. *Science* 220(4598):671–680
- Lee KS, Geem ZW (2005) A new meta-heuristic algorithm for continuous engineering optimization: harmony search theory and practice. *Comput Methods Appl Mech Eng* 194(36–38):3902–3933
- Matsuo M, Kuroda K (1974) Probabilistic approach to design of embankments. *Soils Found* 14(2):1–17
- Morgenstern NRU, Price VE (1965) The analysis of the stability of general slip surfaces. *Geotechnique* 15(1):79–93
- Nguyen VU (1985) Determination of critical slope failure surfaces. *J Geotech Eng* 111(2):238–250
- Onyelowe KC, Iqbal M, Jalal FE, Onyia ME, Onuoha IC (2021) Application of 3-algorithm ANN programming to predict the strength performance of hydrated-lime activated rice husk ash treated soil. *Multiscale Multidiscip Model Exp Des* 1–16
- Phoon K-K, Kulhawey FH (1999) Characterization of geotechnical variability. *Can Geotech J* 36(4):612–624
- Sarma SK (1973) Stability analysis of embankments and slopes. *Geotechnique* 23(3):423–433
- Skempton AW (1948) 'The ϕ 0 Analysis of Stability and Its Theoretical Basis. *Proceedings* 72–77
- Spencer E (1967) A method of analysis of the stability of embankments assuming parallel inter-slice forces. *Geotechnique* 17(1):11–26
- Vanmarcke E (1983) Random fields. *Random Fields* 372
- Wai FAH, Chen WAIFAH (1975) Limit analysis and soil plasticity.
- Wang L, Wu C, Gu X, Liu H, Mei G, Zhang W (2020) Probabilistic stability analysis of earth dam slope under transient seepage using multivariate adaptive regression splines. *Bull Eng Geol Environ* 79(6):2763–2775
- Wang L, Wu C, Tang L, Zhang W, Lacasse S, Liu H, Gao L (2020) Efficient reliability analysis of earth dam slope stability using extreme gradient boosting method. *Acta Geotech* 15(11):3135–3150
- Whitman RV (1984) Evaluating calculated risk in geotechnical engineering. *J GeotechEng* 110(2):143–188
- Wu W (2015) Slope Stability Assessment Based on Limit Analysis. In *Geotechnical Safety and Risk V* (pp. 263–268). IOS Press
- Zhang W, Li H, Li Y, Liu H, Chen Y, Ding X (2021) Application of deep learning algorithms in geotechnical engineering: a short critical review. *Artif Intell Rev* 1–41